Fractal Noise in Quantum Ballistic and Diffusive Lattice Systems

E. J. Amanatidis, D.E. Katsanos and S.N. Evangelou
Department of Physics, University of Ioannina, Ioannina 45110, Greece

We demonstrate fractal noise in the quantum evolution of wave packets moving either ballistically or diffusively in periodic and quasiperiodic tight-binding lattices, respectively. For the ballistic case with various initial superpositions we obtain a space-time self-affine fractal $\Psi(x,t)$ which verify the predictions by Berry for "a particle in a box", in addition to quantum revivals. For the diffusive case self-similar fractal evolution is also obtained. These universal fractal features of quantum theory might be useful in the field of quantum information, for creating efficient quantum algorithms, and can possibly be detectable in scattering from nanostructures.

I. INTRODUCTION

A quantum wave packet $\Psi(x,t)$ evolving from a uniform initial superposition state $\Psi(x,0)$ displays interesting quantum interference phenomena which involve self-affine fractal quantum evolution of the probability densities and quantum revivals. This was shown by Berry [1] in a study of quantum waves confined in boxes by Dirichlet boundary conditions. It was pointed out that the choice of hard wall boundaries introduces quantum fractal noise in the time evolution of uniform deterministic systems obeying the Schrödinger's equation, which is expressed via a self-affine fractal probability density $|\Psi(x,t)|^2$. Moreover, over long periods of time at integer multiples of the revival time T_r, the wave packet $\Psi(x,t)$ returns and reconstructs in its initial form [2]. In a wide class of circumstances the quantum revivals are almost perfect with both space and time periodic $|\Psi(x,t)|^2$.

Most studies are concerned with spectra having a quadratic dependence on the quantum number, such as the simple case of the infinite potential well $E_j = E_1 j^2$, $j = 1, 2, ...$, where perfect and fractional revivals occur at integer and fractional multiples of the revival time T_r, respectively [1]. For quadratic spectra with wave packets localized in energy space around a quantum number $\overline{j}$ the classical time $T_{cl} = \pi\hbar/(E_1\overline{j})$ and the much longer revival time $T_r = \pi\hbar/E_1$ are the only time scales [3]. For more complex energy dispersions, such as the Rydberg states $E_j = E_1/j^2$ $j = 1, 2, ...$ higher order time scales exist apart from the classical, e.g. 1st order, 2nd order, etc, recurrences, as shown for the "return to the origin" probability in the book by Peres [4]. The classical revolution time for a wave packet starting around the $\overline{j}$th orbit is $T_{cl} = \pi\hbar\overline{j}^3/(-E_1)$, while the 1st order recurrences occur at integer multiples of the revival time $T_r = \pi\hbar\overline{j}^4/(-3E_1)$ [2–4]. The classical time scale T_{cl} defines the time up to which the system follows a classical orbit while the revival time scale T_r resembles the Ehrenfest time where the classical Liouville density ceases to describe the system, since quantum interference makes itself obvious with gradual spreading and distortion of the wave packet. The classical and revival times are inversely proportional to the energy eigenvalue separation and its variation, respectively [4]. The full quantum limit $t \to \infty$ is approached for much longer times.

The quantum evolution of wave packets which consist of a large number of simultaneously excited eigenstates is related via the uncertainty principle to ultrashort laser pulses of femtosecond duration. In this way one can study the evolution of a coherent superposition of many quantum states. The quantum evolution of such superpositions can be realised in the physics of Rydberg atoms [5], molecules [6], semiconductor quantum wells [7], mode propagation of Bose-Einstein condensates in magnetic wave guides [8], laser prepared states in ionic traps [9], etc. On the other hand, from studying squeezed wave packets with reduced spatial uncertainty, in order to behave like particles as much as possible, one gains a deep insight into the semi-classical limit where quantum and classical physics meet according to the correspondence principle. The quantum evolution is qualitatively milder than the classical one and it remembers the initial state, due to the reversible and unitary nature of the quantum evolution transformation $\exp(-iHt/\hbar)$. For classical evolution the initial state always converges to a stationary distribution. We show that quantum memory effects exist and a self-affine fractal space and time distribution of the probability density $|\Psi(x,t)|^2$. Quantum revivals also appear in the "return to the origin" probability. They might be interesting for fundamental issues, such as the use of quantum mechanics in computation [10]. It was shown that space-time interference which repeats itself at discrete time intervals can create a subatomic quantum counter [11] and can help towards implementation of factorization for an integer number into primes exploring fractional revivals [12] (see also the N-slit interferometer in [13]).

Our study may also be relevant to another aspect of quantum information theory, which is the newborn subject of quantum random walks (e.g. the Hadamard walk) [14]. A quantum walk is iterated by combining the usual translation with a rotation in "coin"-space, where a quantum coin-flip replaces the classical coin-flip. Of course

one should avoid any measurement at intermediate times [15]. The quantum walk has an improved behavior over the classical random walk since it is characterized by ballistic (quadratic dependence of the mean square displacement in time), instead of the usual diffusive (mean square displacement linear in time) of the classical evolution. It is a general feature of one-particle quantum algorithms to speed up quadratically when compared to classical dynamics [14].

The quantum evolution is analogous to the classical phenomenon of geometrical optics known as the Talbot effect [2]. Talbot inspected a coarsely ruled diffraction grating illuminated with white light through a magnifying lens. When the lens held close to the grating, the rulings appeared in sharp focus, as expected. However, moving the lens away, the rulings of the grating first appeared blurred, as expected, but then reappeared in sharp focus at multiples of a particular distance, known as the Talbot distance. In the Talbot effect the pattern of intensity is doubly periodic, both across the grating and as a function of distance from the grating. More discussion on the Talbot effect and its analogies with the quantum problem can be found in [2]. Although the quantum revivals are semiclassical in nature quantum interference exists since these semiclassical phenomena appear only close to the quantum limit $t \to \infty$.

In this paper, as an alternative to continuous media we aim to study quantum evolution of wave packets moving in tight-binding lattices. A discrete and finite space is important for simulations on a finite computer with the possibility of mapping it to a quantum computer. This study is a general scheme for discetizing space when one deals with linear equations (such as the quantum Schrodinger's equation), which turns out to be particularly useful when the geometry plays an important role. It complies with the necessity to exploit possibilities for the information space, which is also discrete, opposite to the continuous classical phase space. This convenient computational tool for implementing space is favored by the presence of an underlying lattice in solid state applications. We discuss two cases: (i) the ballistic motion in the case of zero site potential where quantum interference from wave scattering at the hard walls creates a sort of quantum "randomness" similarly to that of the "particle in a box", and (ii) a diffusive case via a special quasi-periodic potential of critical strength [16]. It must be stressed that quantum diffusive evolution is very different from classical diffusion although the space fractal dimension of the quantum probability is the same. The spectrum is of the cos type and the stationary eigenstates are simple sin elementary trigonometric functions so that the evolution can be characterized by an infinity of other time scales apart from T_{cl}, T_r. In the ballistic case the motion remains ballistic for all t since the tight binding lattice has no small t semiclassical limit.

Our results confirm the presence of fractal fluctuations of the probability distribution during the ballistic and diffusive quantum evolution, in agreement with Berry [1]. Moreover, for all kinds of quantum noise the fractal noise is described by the predicted universal fractal dimensions D_x, D_t and $D_{x=t}$ of the self-affine curves. For the ballistic motion the mean square distance increases proportionally to the square of the elapsed time while for quantum diffusion the mean square distance increases proportionally to time. The self-affinity seen in the noisy quantum evolution is familiar in non-linear systems. Therefore, techniques from non-linear physics can be used to understand some of the mysteries of quantum mechanics, particularly quantum evolution in open systems in the presence of time-dependent potentials.

II. BALLISTIC QUANTUM EVOLUTION

A. Space-time structures

We have created space-time structures on the discrete orthonormal finite lattice space basis $\{|x\rangle, x = 1, 2, ..., N\}$ for various continuous times t. For the ballistic quantum evolution in a line the mean-square displacement grows quadratically $\langle x^2 \rangle = 2t^2$. It can be expressed via the stationary eigensolutions of the Hamiltonian H through the evolution operator $\exp(-iHt/\hbar)$, since H is time-independent. The static Schrodinger's equation $H|j\rangle = E_j|j\rangle$, $j = 1, 2, ..., N$ corresponding to the matrix H, which is tridiagonal for a one-dimensional lattice with zero diagonal entries and constant off-diagonal elements, has stationary eigenvalues, eigenvectors $E_j = 2\cos\frac{j\pi}{N+1}$, $|j\rangle = \sqrt{\frac{2}{N+1}}\sum_{x=1}^{N}\sin\frac{j\pi x}{N+1}\,|x\rangle$. The quantum evolution of the initial ket $|\Psi(0)\rangle$ can be expressed as

$$\begin{aligned}|\Psi(t)\rangle &= e^{-iHt/\hbar}|\Psi(0)\rangle \\ &= \sum_{j=1}^{N} e^{-iE_jt/\hbar}|j\rangle\langle j|\Psi(0)\rangle \end{aligned} \quad (1)$$

so that the space-time wave function reads

$$\begin{aligned}\Psi(x,t) &= \langle x|\Psi(t)\rangle \\ &= \sum_{j=1}^{N} e^{-iE_jt/\hbar}c_x^{(j)}\langle j|\Psi(0)\rangle, \end{aligned} \quad (2)$$

with the the amplitude on site x denoted by the elementary trigonometric function $c_x^{(j)} = \langle x|j\rangle = \sqrt{\frac{2}{N+1}}\sin\frac{j\pi x}{N+1}$.

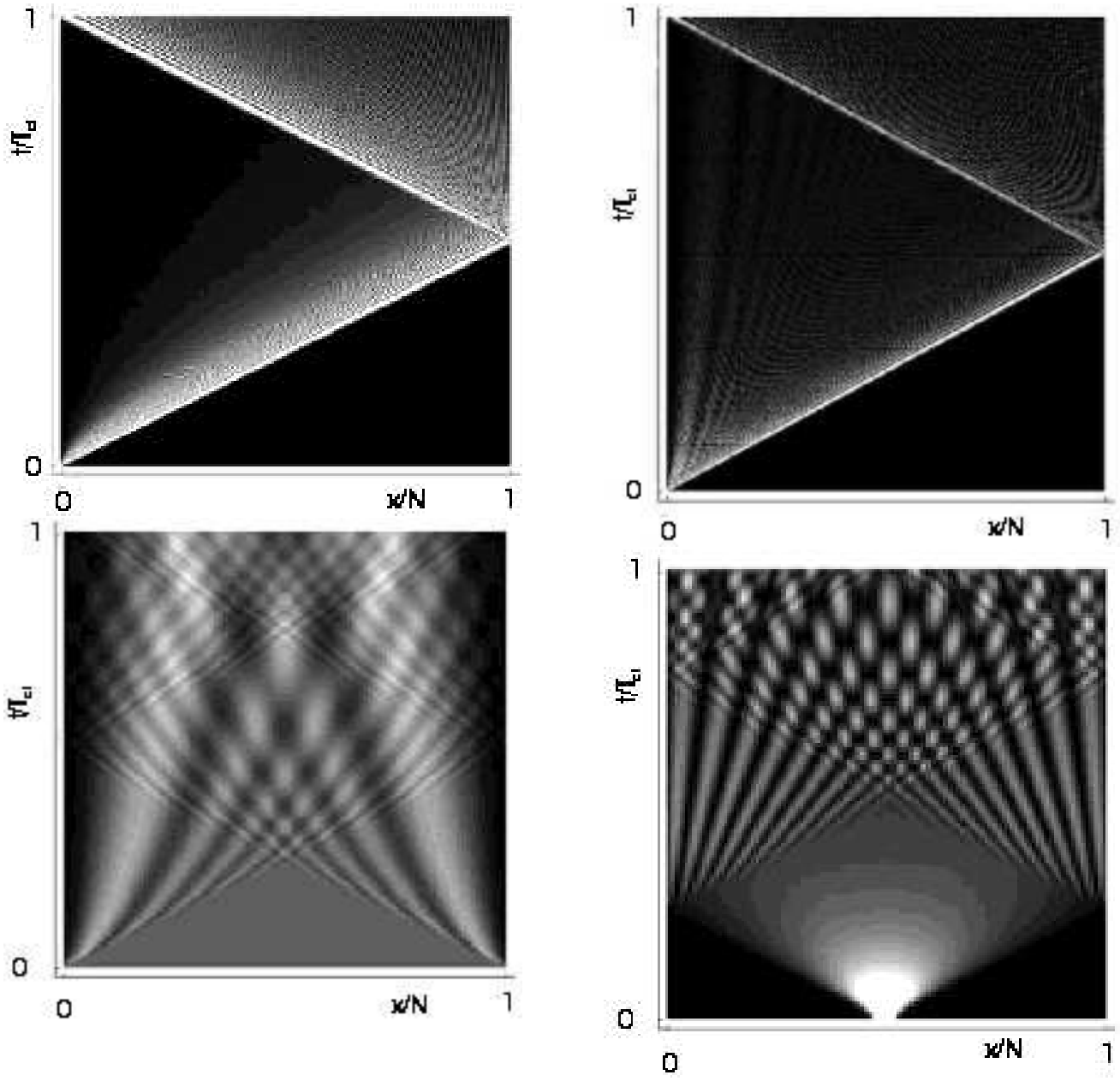

Fig. 1. The space-time (x-t) representation of various initial wave packets moving ballistically in a chain. The classical time is $T_{cl} \approx \hbar(N+1)$ and quantum memory effects are seen to develop with different initial wave packets giving different pictures. **(a)** For a local initial state $\Psi(x, t=0) = \delta_{x,1}$ in position 1 with $N = 1000$ we see almost classical motion with recurrence at $t = 1001$. **(b)** For a spatially uniform initial superposition $\Psi(x, t=0) = 1/\sqrt{N}$ in a chain with $N = 100$ we observe interesting interference effects. **(c)** For an initial uniform superposition of all stationary eigenstates with $|\Psi(0)\rangle = \sum_{j=1}^{N} a_j |j\rangle$, with $a_j = 1/\sqrt{N}$ for any j, we have $\Psi(x, t=0) = \sqrt{2/N(N+1)} \sum_{j=1}^{N} \sin \frac{j\pi x}{N+1}$ amplitude at site x for a chain with $N = 1000$. The result resembles that of (a) where a wave is released at one end of the chain since in the spatial basis this initial state has higher amplitude near the end of the chain with diminishing oscillations. **(d)** For a Gaussian in space initial

superposition $\Psi(x,t=0)=a_x$ for $N=100$ interesting interference patterns are also seen.

The ballistic evolution is considered for various initial superpositions $\Psi(x,0) = \langle x|\Psi(0)\rangle$, chosen from expansions either in the spatial basis with $|\Psi(0)\rangle = \sum_{x=1}^{N} a_x|x\rangle$, $\sum_{x=1}^{N}|a_x|^2 = 1$ or in the eigenstate basis with $|\Psi(0)\rangle = \sum_{j=1}^{N} a_j|j\rangle$, $\sum_{j=1}^{N}|a_j|^2 = 1$. The amplitude $c_x^{(j)}$ is real and the transformation from the spatial $|x\rangle$ to the eigenstate $|j\rangle$ basis or its inverse from $|j\rangle$ to $|x\rangle$ are the same. In this case the computations of the space-time wave function $\Psi(x,t)$ at various times are particularly simple by replacing the eigenvalues E_j, eigenvector amplitudes c_x^j in Eq. (2). For initial superposition in the spatial basis the normalized space-time probability becomes

$$P(x,t) = |\Psi(x,t)|^2 = \left|\sum_{j=1}^{N} e^{-iE_j t/\hbar}(\sum_{x'=1}^{N} c_{x'}^{(j)*} a_{x'})c_x^{(j)}\right|^2 \quad (3)$$

and for superposition in the eigenbasis the normalized space-time probability is

$$P(x,t) = |\Psi(x,t)|^2 = \left|\sum_{j=1}^{N} e^{-iE_j t/\hbar} c_x^{(j)} a_j\right|^2 . \quad (4)$$

Firstly, the initial wave was released on a *local* state at one end of the chain with $|\Psi(0)\rangle = |1\rangle \Rightarrow \Psi(x,0) = \langle x|\Psi(0)\rangle = \delta_{x,1}$ which from Eq. (3) at later times gives the probability

$$P(x,t) = |\Psi(x,t)|^2 = \left|\sum_{j=1}^{N} e^{-iE_j t/\hbar} c_1^{(j)*} c_x^{(j)}\right|^2 , \quad (5)$$

in terms of the eigenvalues E_j, eigenvectors $|j\rangle = \sum_{x=1}^{N} c_x^{(j)}|x\rangle$. This gives an almost classical evolution of a point particle seen in Fig. 1(a) where the particle at time $T_{cl} = \hbar(N+1)$ returns to its initial position. The quantum revival resembles a classical particle moving with constant velocity which reflects at the boundaries at $t = T_{cl}$ and returns to its original position 1. Our second initial choice was the spatial superposition in space $|\Psi(0)\rangle = \sum_{x=1}^{N} a_x|x\rangle$ with *uniform* $a_x = 1/\sqrt{N}$ for all x, which gives from Eq. (3) the normalized space-time probability

$$P(x,t) = |\Psi(x,t)|^2 = \frac{1}{N}\left|\sum_{j=1}^{N} e^{-iE_j t/\hbar} \sum_{x'=1}^{N} c_{x'}^{(j)*} c_x^{(j)}\right|^2 . \quad (6)$$

The corresponding space-time structure which arises from the initial condition of Eq. (6) is shown in Fig. 1(b) where we can observe interesting quantum interference features. The third choice we have made was not spatial but a *uniform expansion on all stationary eigenstates* $|j\rangle$ choosing the initial superposition $|\Psi(0)\rangle = \sum_{j=1}^{N} a_j|j\rangle$, with $a_j = 1/\sqrt{N}$ for all j. If transformed to the spatial basis this choice has a maximum at one end of the chain with decaying oscillations. At later times the normalized space-time probability is

$$P(x,t) = |\Psi(x,t)|^2 = \frac{1}{N}\left|\sum_{j=1}^{N} e^{-iE_j t/\hbar} c_x^{(j)}\right|^2 . \quad (7)$$

Finally, a *Gaussian* spatial initial superposition was chosen of the type $|\Psi(0)\rangle = \sum_{x=1}^{N} a_x|x\rangle$, centered in the middle of the chain $N/2$. In this case after normalization the probability amplitude can be obtained from Eq. (3) with $|a_x|^2 \propto e^{-(x-N/2)^2/(2\sigma^2)}$, $\sum_{x=1}^{N}|a_x|^2 = 1$, drawn from a Gaussian with $\sigma^2 = 1$.

The obtained space-time structures for the various initial from the second to the fourth conditions are shown in Fig. 1. The white denotes high amplitude and the amplitude is lower in the darker. The spectacular patterns shown are known as quantum carpets [2] and arise from scattering at the hard walls at the ends. The quantum intereference is more prominent for the uniform initial condition (Fig. 1(b)) where the picture resembles more closely the quantum carpets of Berry [1]. We can also see quantum recurrences more clearly in Fig. 1(a), (c) where the initial wavepacket has maximum amplitude close to the end site 1. The quantum carpets shown in Fig. 1. repeat indefinitely at time T_{cl}, but less and less less accurately each time.

B. Fractal dimensions for the probability density

We observe the quantum evolution for a uniform initial wave function along the chain as a function of space freezing the time, as a function of time at a single site or varying space positions equal to time. The corresponding pictures are shown in Figure 2 where interesting self-affine fractal oscillations are seen. For the spatial distribution our simple computations for the fractal dimension coincide with the value $D_x = 1.5$ predicted by Berry. This value coincides with the displacement curve of classical random walks which gives Brownian noise. Quantum "randomness" described by the fractal dimension D_x arises from the linear Schrodinger's equation, only due to quantum interference from scattering at the boundaries. It must be noted these curves are not self-similar but self-affine fractals. The computed time fractal dimension also gives the predicted value $D_t = 1.75$. The D_t is higher than D_x as it can be seen form the more noisy oscillating of the probability density as a function of time t. We also display a space-time function along the diagonal $x = t$

where the self-affine fluctuations are much smaller with $D_{x=t} = 1.25$.

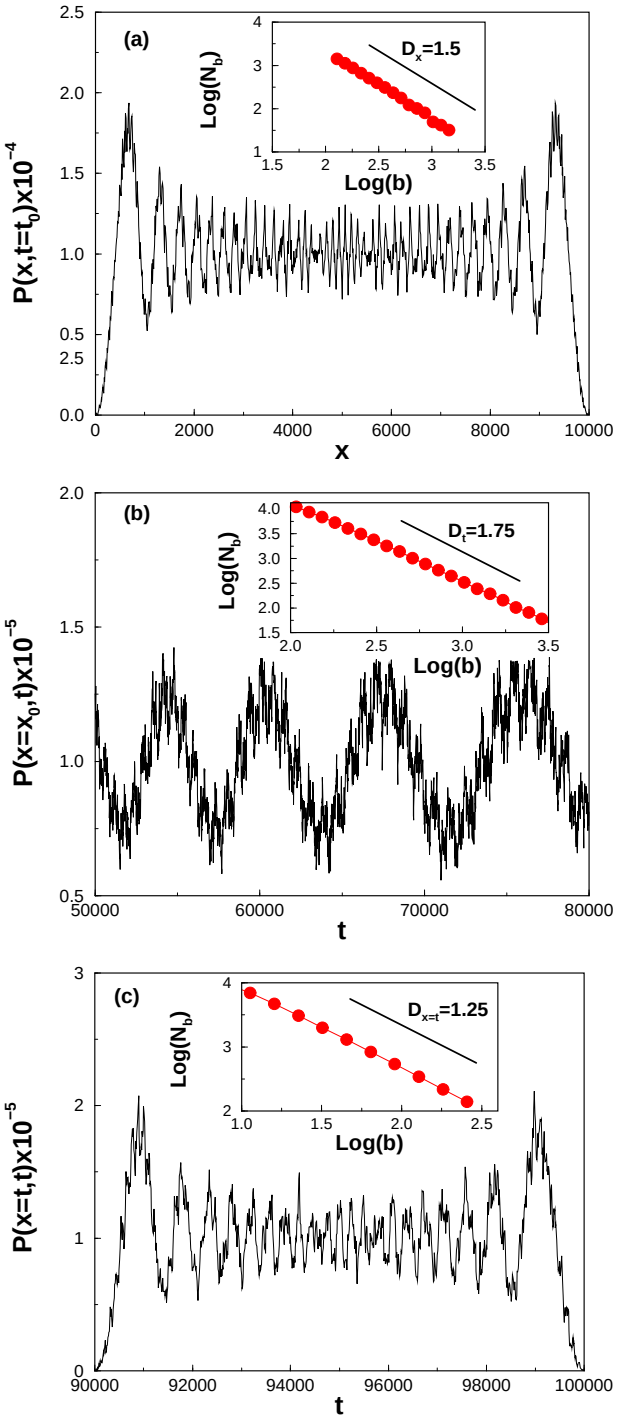

Fig. 2. Fractal noise of an initially uniformly distributed in space wave packet for a chain of length $N = 10000$. **(a)** The absolute of the probability amplitude squared $|P(x,t)|^2$ as function of space x at fixed time $t_0 = 100000$. **(b)** A function of time t at the fixed site $x_0 = 5000$. **(c)** A function of both space and time with $x = t$. The obtained fractal dimensions are denoted in the log-log insets on the plot.

The capacity (box) dimension of the self-affine $y = y(x)$ curves is computed by counting boxes of linear size $b.\tau$ along the x-axis axis and of size $b.a$ along the y-axis. It must be noted that a similarity dimension cannot be defined since for a self-affine curve scaling is different along the two axes. We have used integer time units so the minimum box width along the x-axis is taken $\tau = 1$ and use a high-resolution grid for the amplitude along the y-axis. This is required in order to obtain the "local" non-integer fractal dimension D of the self-affine curves, while larger values of a finally give the well known "global" fractal dimension $D = 1$ [17]. The selected values of a were of order of 10^{-10} for both the space D_x and time D_t dimensions. For the space-time fractal a is of the order of 7×10^{-8}. The box dimension is defined by the scaling equation $N(b,a) \sim b^{-D}$, where N is the number of boxes needed to cover the curve [17]. A linear fit of the scaling equation is displayed in the log-log plots of the corresponding insets of Fig.2 which gives D from the slope. As pointed out above the obtained results for $D_x, D_t, D_{x=t}$ are in agreement with the values for the fractal dimensions predicted by Berry [1]. For the other initial conditions considered we find similar fractal dimensions although with errors arising from the small sizes (see Fig. 3).

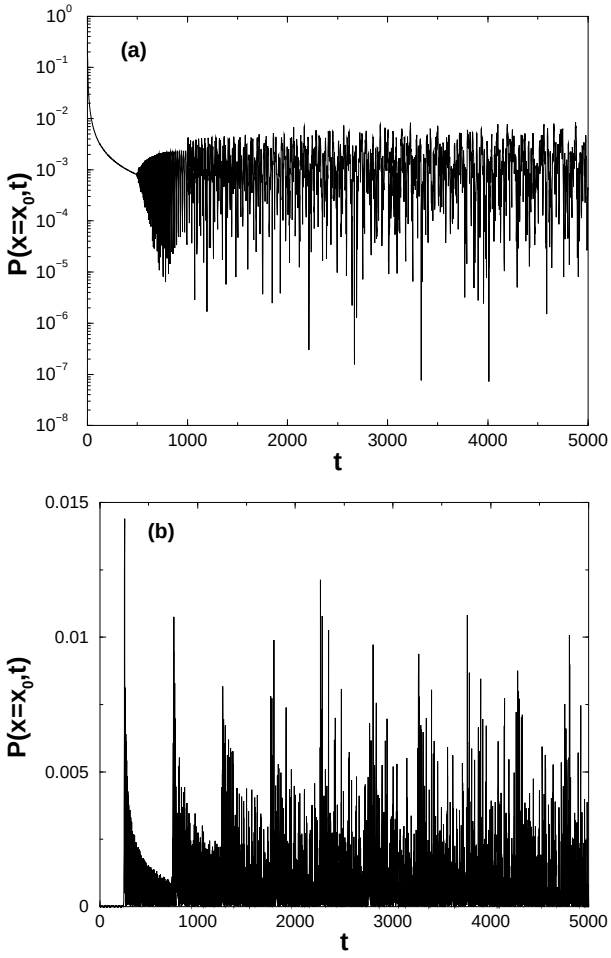

Fig. 3. Time fractals for other initial conditions in a chain of

length $N = 1000$. **(a)**. A Gaussian spatial superposition at a fixed site $x_0 = 500$ where we compute $D_t \approx 1.80$. **(b)** A uniform initial superposition in the eigenbasis where we find $D_t \approx 1.46$.

C. "Return to the origin" probability

The "survival" or "return to the origin" probability is defined from the squared absolute amplitude overlap

$$P_0(t) = |\langle\Psi(0)|\Psi(t)\rangle|^2 \tag{8}$$

which can be computed from Eq. (1). For an initial superposition in the spatial basis $|\Psi(0)\rangle = \sum_{x=1}^{N} a_x|x\rangle$ one obtains

$$P_0(t) = \left|\sum_{j=1}^{N}\sum_{x=1}^{N}\sum_{x'=1}^{N} e^{-iE_j t/\hbar} a_x^* a_{x'} c_{x'}^{(j)*} c_x^{(j)}\right|^2 . \tag{9}$$

For an initial superposition in the eigenstate basis $|\Psi(0)\rangle = \sum_{j=1}^{N} a_j|j\rangle$ we have the simpler expression independent of eigenvectors

$$\begin{aligned} P_0(t) &= \left|\sum_{j=1}^{N} |a_j|^2 e^{-iE_j t/\hbar}\right|^2 \\ &= \sum_{j=1}^{N}\sum_{j'=1}^{N} |a_j|^2 |a_{j'}|^2 e^{-i(E_j - E_{j'})t/\hbar}. \end{aligned} \tag{10}$$

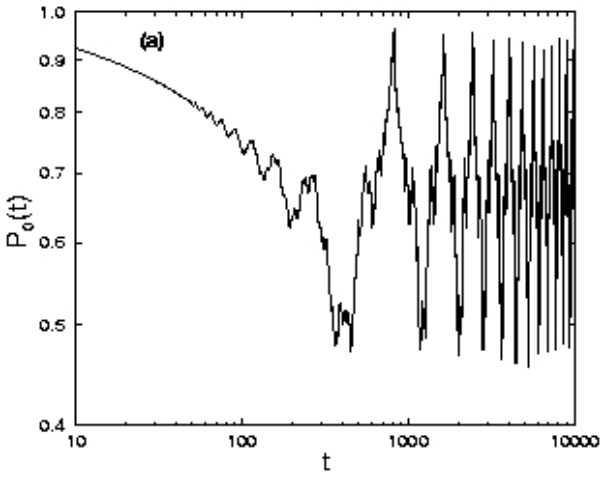

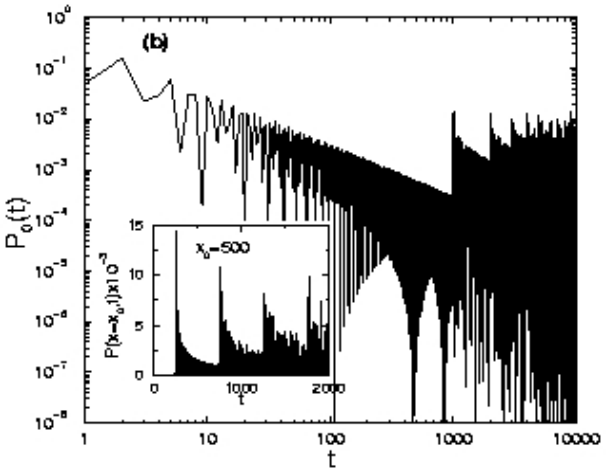

Fig. 4. The "return to the origin" probability $P_0(t)$. **(a)** For an initially uniform superposition in space and a chain of length $N = 100$. The quantum revivals occur at an estimated period $T_r \propto \hbar(N+1)^2 \approx 0.08(N+1)^2$. **(b)** For an initially uniform superposition of stationary eigenstates in a chain of length $N = 1000$. In the inset a presentation of the probability density $P(x,t)$. The quantum revivals which appear with period $T_{cl} \propto \hbar(N+1)$.

The quantum revivals can be seen in Fig.4 where $P_0(t)$ is shown versus t in a log-log plot. $P_0(t)$ is periodic in the early stages of evolution which becomes less clear later. The long-time overall asymptotic algebraic decay $P_0(t) \propto \frac{1}{t}$ of ballistic systems can be seen predicted from properties of Bessel functions. Fractional revivals with smaller strength are also seen. In the eigenbasis the expansion of the states j around the center of the wave packet $\overline{j}$ $E_j = E_{\overline{j}} + (j-\overline{j})\frac{\partial E_{\overline{j}}}{\partial \overline{j}} + \frac{1}{2!}(j-\overline{j})^2 \frac{\partial^2 E_{\overline{j}}}{\partial^2 \overline{j}} + ... = E_{\overline{j}} + 2\pi\hbar[-\frac{(j-\overline{j})}{T_{cl}} + \frac{(j-\overline{j})^2}{2!T_r} - ...]$ allows to find the time scales $T_{cl} = \hbar(N+1)/\sin(\overline{j}\pi/(N+1))$, $T_r = \hbar(N+1)^2/(\pi\cos(\overline{j}\pi/(N+1)))$, etc. Of course, if $|\Psi(0)\rangle$ consists of only one eigenstate with $j = \overline{j}$ the system shows no evolution. When the wave packets consists of many states j near the band center $E \approx 0$ then the dominant time scale is $T_{cl} \propto \hbar(N+1)$ with $T_r = \infty$. When it consists of states j near the edges $E \approx \pm 2$ then $T_{cl} = \infty$ so the dominant time scale is $T_r \propto \hbar(N+1)^2$. In Fig. 4(a) for a uniform expansion in the spatial basis we observe period proportional to T_r since it correspond to eigenstates close to $E \approx \pm 2$. In Fig. 4(b) the uniform distribution in the eigenbasis emphasises states from the band center $E \approx 0$ which is the mean energy for this initial superposition, so that we observe a period proportional to T_{cl}.

III. DIFFUSIVE QUANTUM EVOLUTION

We have also considered a chain with non-zero site potential taking the quasi-periodic value $\epsilon_x =$

$2cos(2\pi xM/N)$, $x = 1, 2, ..., N$ for M, N successive Fibonacci numbers so that the rational M/N approaches the inverse golden mean ratio. In this critical case one obtains diffusive time evolution with the mean-square-displacement growing linearly with time $\langle x^2 \rangle \propto t$ which can be compared with the ballistic case $\langle x^2 \rangle \propto t^2$ studied in Chapter II. It must be stressed again that although diffusive this is quantum evolution and not classical.

A. Space-time structures

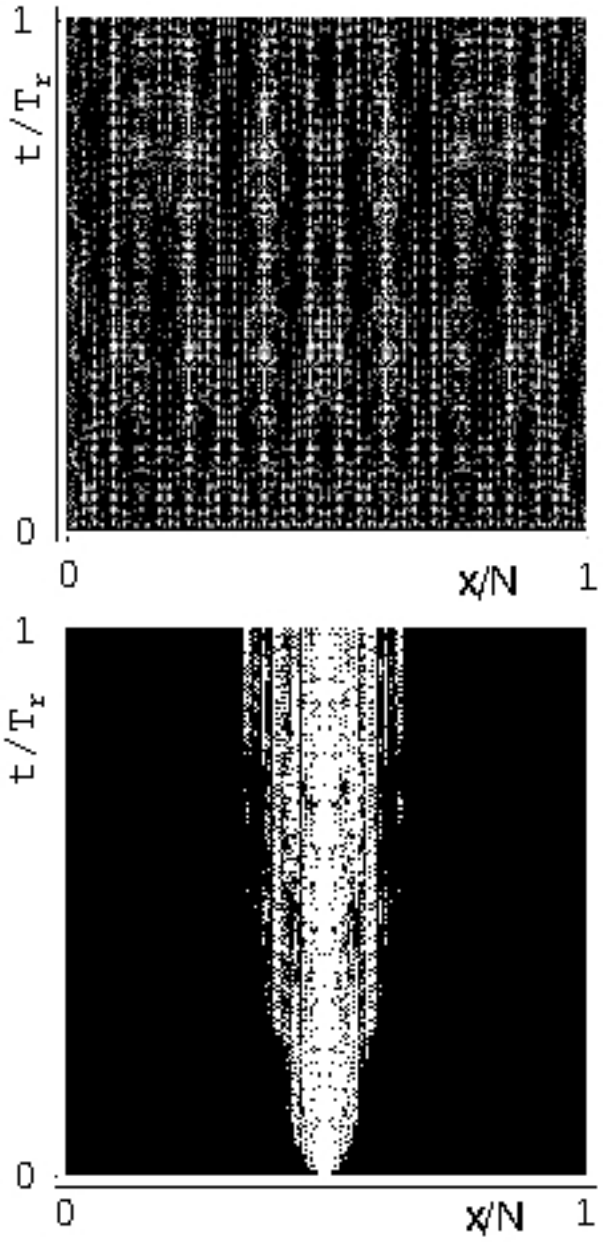

Fig. 5. The space-time $(x - t)$ representations for quantum diffusive evolution in a quasiperiodic chain of length $N = 987$. **(a)** For an initially uniform distributed wavepacket in space as a function of space x and time t. **(b)** For an initially Gaussian wave packet in space.

The obtained space-time structures for the diffusive case and two spatial initial conditions are shown in Fig. 5. Again, the white colour denotes high amplitude and the darker lower amplitude. The figures show spectacular patterns due to quantum intereference from scattering at the hard walls at the ends of the chains but no quantum revivals. We show the space-time evolution for a uniform (Fig. 5(a)) and Gaussian spatial wave packet (Fig. 5(b)). The quantum interference gives very different results in this case since the obtained quantum carpets display self-similarity superimposed on the self-affinity found for ballistic evolution. For the Gaussian in space initial state Fig. 5(b) we see slow quantum evolution with the system not reaching the boundary within T_{cl}.

B. Fractal dimensions for the probability density

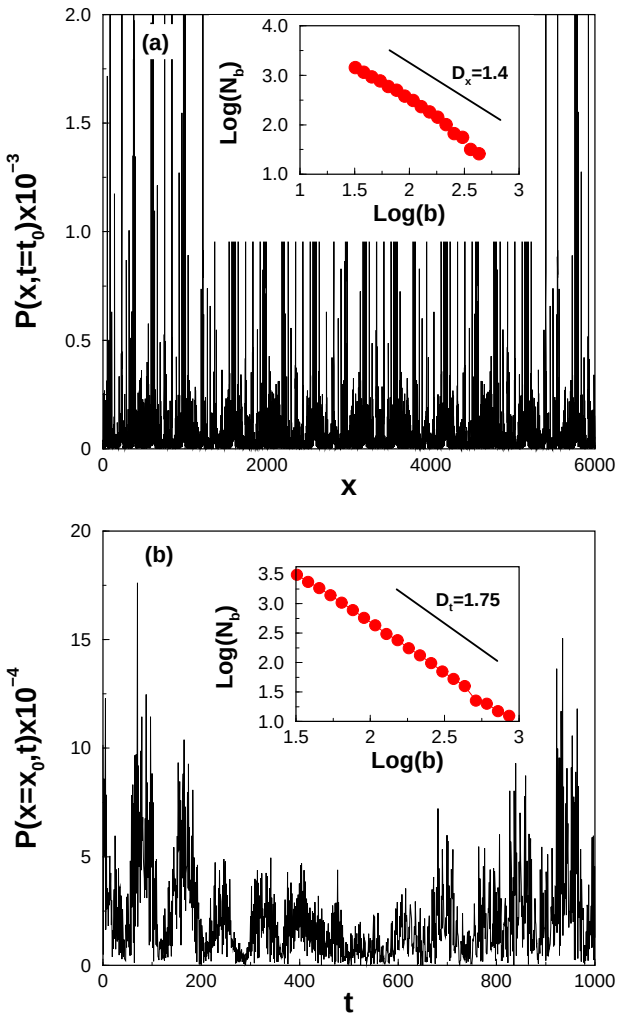

Fig. 6. Fractal noise for diffusion in a chain of length $N = 987$. **(a)** An initially uniform wave packet at time $t = 10$ as a function of space. **(b)** As function of time at site $x_0 = 500$.

We obtain similar to ballistic case self-affine fractal dimensions displayed in Fig. (6). Apart from self-affine the curves are also self-similar fractals with dimensions defined in [16]. From the normalized probability measure $P(x,t)$ with $\sum_{x=1}^{N} P(x,t) = 1$ we compute $-\sum_{x=1}^{N} P(x,t) \ln P(x,t)$, $\ln \sum_{x=1}^{N} P(x,t)^2$ and from the linear fits vs. $\ln N$ obtain the space fractal dimensions D_1^x, D_2^x, respectively. Our results gave give the entropy fractal dimension $D_1^x \approx 0.85$ for the uniform and ≈ 0.43 for the Gauss while for the correlation dimension we obtain $D_2^x \approx 0.77$ for the uniform and ≈ 0.37 for the Gauss. It must be pointed out that the fractal dimensions D_1, D_2 depend strongly on initial conditions (see Fig. 7).

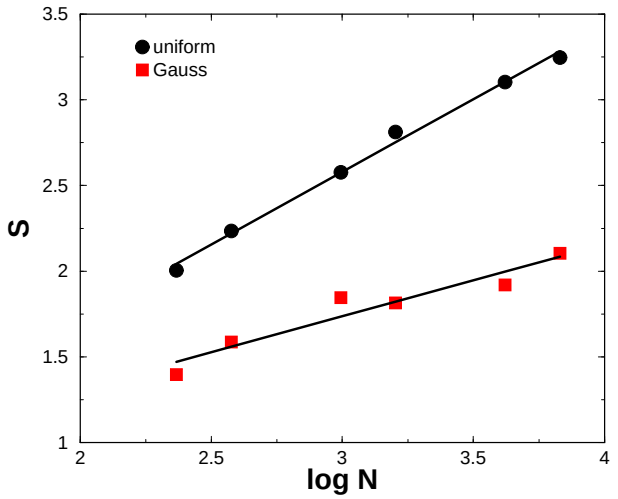

Fig. 7. Entropy vs. $logN$ for the diffusive model for an initially **(a)** uniform and **(b)** gauss distribution, both in space. The information dimension $D_1^x \approx 0.85$ for the uniform and $D_1^x \approx 0.43$ for the Gauss is obtained form the slopes of the linear fits. Similar results exist for the correlation dimension D_2.

C. "Return to the origin" probability

The "return to the origin" probability now shows many fluctuations and if we define the time integrated correlation function $C(t) = (1/t)\int_0^t P_0(t')dt'$ vs. t. We also observe the long-time asymptotically algebraic overall decay $P_0(t) \propto \frac{1}{\sqrt{t}}$ known for diffusive systems.

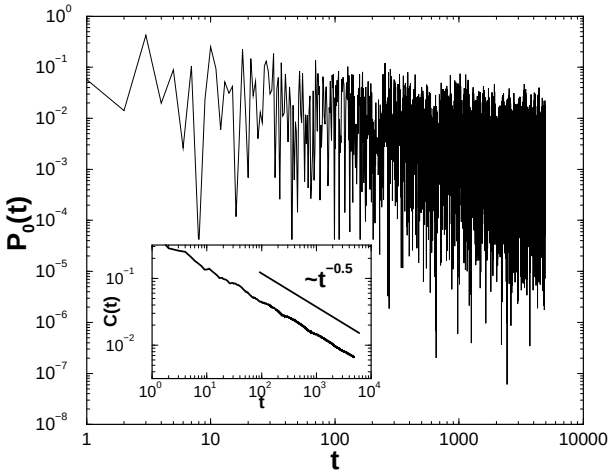

Fig. 8 . The "return to the origin probability" for an initially uniform distributed wavepacket in a chain of length $N = 987$. The inset shows the log-log scale of the correlation function $C(t)$ vs. t with diffusive correlation behavior.

IV. DISCUSSION-CONCLUSIONS

We studied the milder when compared to classical quantum ballistic and diffusive evolution of wave packets. It is different from that of classical point particles, nevertheless, shows fractal noise in the form of self-affine curves. Our calculations are done by discretizing the space into a tight-binding chain lattice. For the ballistic case semiclassical diffusive evolution does not exist for small t, to cross over to ballictic for longer times [18], since the ballistic law is satisfied for all t. In this case we display quantum memory effects by observing different evolutions for various initial superposition wave packets $\Psi(x,t)$. However, in agreement with Berry's findings for a "particle in box" a self-affine fractal space-time $P(x,t) = |\Psi(x,t)|^2$ is found. For diffusive systems the evolution apart from self-affine is also self-similar with no recurrences.

The quantum evolution could be efficiently implemented by a quantum computer so that one can use the simulation to solve certain computational tasks by creating more efficient algorithms. In fact, $P_0(t)$ can reveal the prime factors of an encoded number [12]. On the other hand, fractals known from non-linear physics also appear in quantum physics, despite the fact that quantum mechanics is linear. The space fractal dimension $D_x = 1.5$ obtained for the spatial distribution corresponds to Brownian $1/f^2$ noise familiar from random walks. Therefore, techniques can be transferred from non-linear physics to quantum mechanics and vice versa. Finally, quantum intereference can make itself obvious in scattering from nanostructures, such as carbon nanotubes. It can possibly influence the temperature inde-

pendent white noise known as "shot noise" for measurements of current in nanostructures [19].

In summary, classical systems are diffusive due to either non-linear effects, which may lead to deterministic chaos, or introduced randomness from outside (flipping a coin) as for the random walk. In these cases irreversibility naturally arises with convergence to a Gaussian steady state distribution for any initial state. In quantum systems the evolution is smoother, wave-like, reversible, with no convergence to a steady state, since quantum memory develops. However, we show for simple lattice systems fractal noise due to quantum interference from scattering at the boundaries. The noisy quantum evolution seems not only independent of chaos but is present for all kinds of evolution.

[1] M.V. Berry, J. Phys. **A 26**, 6617 (1996).

[2] Michael Berry, Irene Marzoli and Wolfgang Schleich, *"Quantum Carpets, carpets of light"*, Physics World, pg. 39, June (2001).

[3] D.L. Aronstein and C.R. Stroud Jr, Phys. Rev. A **55**, 4526 (1997). W. Loinaz, I.J. Neumann, quant-ph/9902039.

[4] A. Peres, *"Quantum theory: Concepts and Methods"*, Klwer Academic Publishers (1995).

[5] J.A. Yeazell and C.R. Stroud Jr, Phys. Rev. **A 43**, 5153 (1991).

[6] M.J.J. Vrakking, D.M. Villeneuve and A. Stolow, Phys. Rev. **A 54**, R37 (1996).

[7] F. Steininger *al et al*, Phys. Rev. Lett. **77**, 550 (1996).

[8] A.E. Leanhardt *et al*, Phys. Rev. Lett. **89**, 040401 (2002).

[9] D.M. Meekhof, C. Monroe, B.E. King, W.M. Itano and D.J. Wineland, Phys. Rev. Lett. **76**, 1796 (1996).

[10] M.A. Nielsen and I.L. Chuang, *"Quantum Computation and Quantum Information"*, Cambridge University Press, Cambridge (2000). See also a list of relevant references in the lecture course *"Introduction to Quantum Computing"* by S.N. Evangelou at http://www.lancaster.ac.uk/users/esqn/man2002.

[11] W.G. Harter, Phys. Rev. A **64**, 012312 (2001).

[12] H. Mack, M. Bienert, F. Haug, M. Freyberger and W.P. Schleich, Phys. Stat. Sol. **(b) 233**, No. 3. 408 (2002).

[13] J.F. Clauser and J.P. Dowling, Phys. Rev. A **53** 4587 (1996).

[14] Y. Aharonov, L. Davidovich and N. Zagury, Phys. Rev. A **48(2)**, 1687 (1993).

[15] For an introductory review to *quantum random walks* see: J. Kempe, quant-ph/0303081.

[16] S.N. Evangelou and D.E. Katsanos, J. Phys A: Math. Gen. **26**, L1243 (1993).

[17] J. Feder, *"Fractals"*, Plenum Press, New York (1998).

[18] D.K. Wójcik and J.R. Dorfman, Phys. Rev. Lett. **90**, 230602 (2003).

[19] Y.M. Blanter and M. Buttiker, Phys. Rep. 336 (2000).